

Complementary silicide source/drain thin-body MOSFETs for the 20nm gate length regime

Jakub Kedzierski[†], Peiqi Xuan, Erik H. Anderson[‡], Jeffrey Bokor, Tsu-Jae King, Chenming Hu

Department of Electrical Engineering and Computer Sciences, University of California at Berkeley, Berkeley CA, 94720 USA

[‡]Lawrence Berkeley National Laboratory, Berkeley CA

[†]E-mail: jakub@eecs.berkeley.edu, Tel:510-643-2639, Fax:510-643-2636

Abstract

Thin-body transistors with silicide source/drains were fabricated with gate-lengths down to 15nm. Complementary low-barrier silicides were used to reduce contact and series resistance. Minimum gate-length transistors with $T_{ox}=40\text{\AA}$ show PMOS $|I_{dsat}|=270\mu\text{A}/\mu\text{m}$ and NMOS $|I_{dsat}|=190\mu\text{A}/\mu\text{m}$ with $V_{ds}=1.5\text{V}$, $|V_g-V_t|=1.2\text{V}$ and, $I_{on}/I_{off}>10^4$. A simple transmission model, fitted to experimental data, is used to investigate effects of oxide scaling and extension doping.

Introduction

The single[1] and double[2] gate thin-body transistors are promising device designs for the 5-50nm gate-length regime. One of their major challenges is the large series resistance of the thin body layer. In this paper we present a method for reducing this resistance with the use of dual low-barrier silicide source/drains: PtSi for PMOS, and $\text{ErSi}_{1.7}$ for NMOS, **Fig. 1**. In previous studies, bulk-Si silicide source/drain MOSFETs[3] have exhibited large leakage currents. Our use of a thin body reduces leakage by orders of magnitude. This symbiotic relationship between leakage suppression by the thin-body structure and the low series resistance of the silicide source/drain structure results in a promising device technology that can be scaled down to 15nm gate-length. It also provides an alternative to the elevated source/drain approach as a general method for reducing series resistance of thin-body designs.

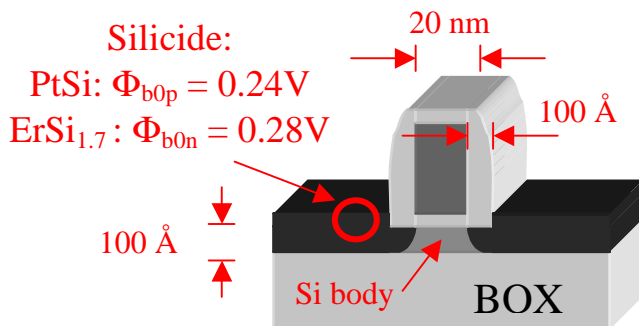


Figure 1: The thin-body silicide source/drain MOSFET in cross section. Source/drains are made in 100Å Si: NMOS uses $\text{ErSi}_{1.7}$ ($\Phi_{b0n}=0.28\text{V}$), PMOS uses PtSi ($\Phi_{b0p}=0.24\text{V}$). Spacer thickness is limited to 100Å, in order to guarantee that the metal diffuses underneath the gate.

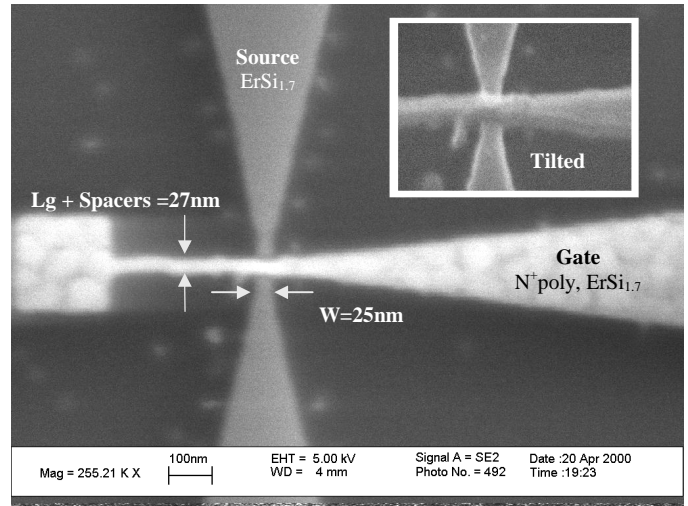


Figure 2: SEM image of an $\text{ErSi}_{1.7}$ device with a polysilicon gate length of 15nm and two 6nm SiO_2 spacers. Device width is 25nm.

Device Fabrication

A lightly doped ($N_a=1\text{E}15\text{ cm}^{-3}$), 100nm thick, silicon on insulator (SOI) film was thinned to 140Å using a two step thermal oxidation. The mesa was defined using a calixarene/G-line double exposure process. Optical exposure of coarse features in G-line resist was followed by 100keV e-beam lithography of fine features in calixarene resist and a dry etch. The gate stack consisted of a 40Å thermal gate oxide, a 550Å *in-situ* doped N-type polysilicon gate, and a 150Å deposited SiO_2 hard mask. Gate lithography also involved a calixarene/G-line double exposure process aligned to the previous layer using SiGe alignment marks. Following gate formation, 100Å SiO_2 spacers were formed. A HF-last clean was performed just prior to metal deposition, and SOI thickness was measured to be 85~100Å. PMOS devices received 75Å of Pt evaporated in an e-beam evaporator. PtSi was formed with a 400°C 1h anneal in a N_2 ambient. Unreacted Pt was then removed in a dilute Aqua Regia etch. NMOS devices received 70Å of Er evaporated in a UHV e-beam evaporator with the base pressure of the oxidizing ambient kept below 10^{-10} torr. $\text{ErSi}_{1.7}$ was formed using a 400°C 1h UHV anneal, and unreacted Er was then removed in a dilute nitric acid etch. **Fig. 2** shows an NMOS device with $L_g=15\text{nm}$. Neither NMOS nor PMOS devices used any significant doping in the source, drain, or body.

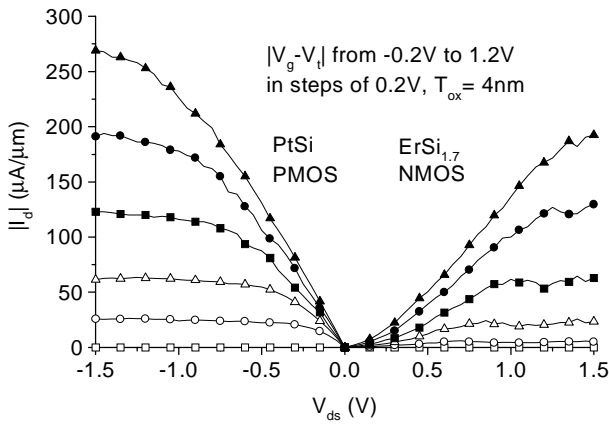


Figure 3.4: I-V characteristics of the minimum gate-length devices. For the **PMOS transistor**, $L=20\text{nm}$, $I_{\text{dsat}}=270\mu\text{A}/\mu\text{m}$ at $V_{\text{ds}}=1.5\text{V}$ and $|V_{\text{g}}-V_{\text{t}}|=1.2\text{V}$. Swing is $100\text{mV}/\text{dec}$, $I_{\text{on}}/I_{\text{off}}=5\text{E}5$, and $V_{\text{t}}=-0.7\text{V}$. For the **NMOS transistor**, $L=15\text{nm}$, $I_{\text{dsat}}=190\mu\text{A}/\mu\text{m}$ at $V_{\text{ds}}=1.5\text{V}$ and $|V_{\text{g}}-V_{\text{t}}|=1.2\text{V}$. Swing is $150\text{mV}/\text{dec}$, $I_{\text{on}}/I_{\text{off}}=1\text{E}4$, and $V_{\text{t}}=-0.1\text{V}$.

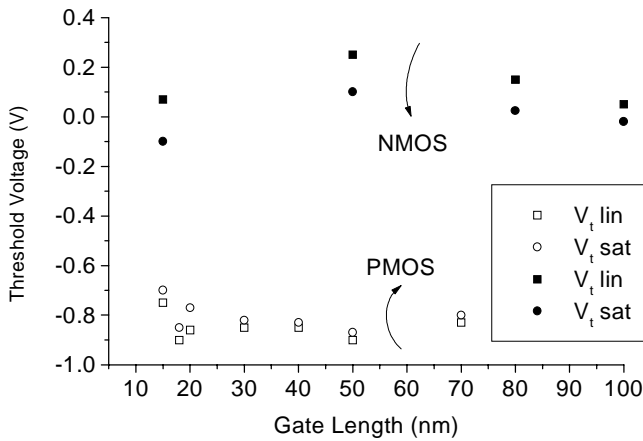
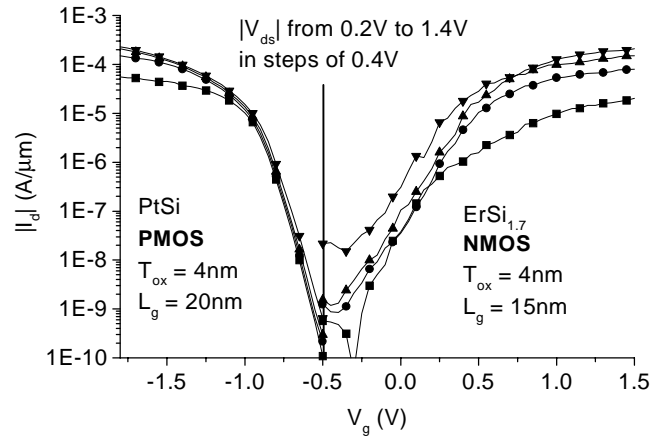


Figure 5: Linear and saturation threshold voltages as a function of gate length for both NMOS and PMOS.

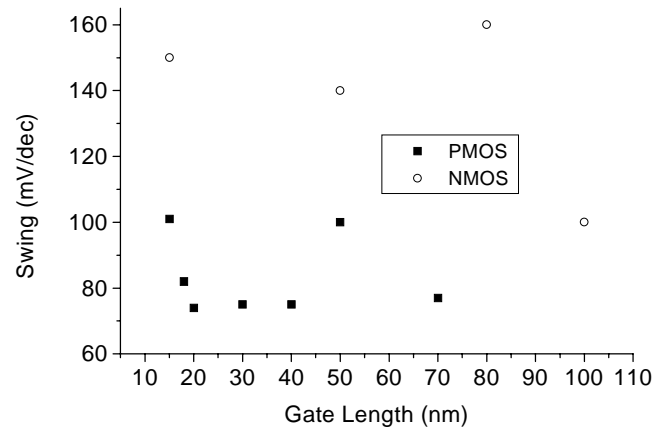


Figure 6: Swing dependence on gate length. For PMOS devices $S=75\text{mV}/\text{dec}$ down to 20nm gate lengths. NMOS devices show a larger variation in swing with $S=100\text{--}160\text{mV}/\text{dec}$.

Device Characterization

Fig. 3.4 show the I-V characteristics of the minimum gate-length transistors. The PtSi PMOS transistor has a 20nm gate length, and $I_{\text{dsat}}=270\mu\text{A}/\mu\text{m}$ with $T_{\text{ox}}=40\text{\AA}$ at $|V_{\text{ds}}|=1.5\text{V}$. Sub-threshold characteristics show excellent short-channel effects, and a V_{t} of -0.7V . The abnormally high V_{t} is due to the N^+ poly gate, it can be reduced using a mid-gap gate material such as P^+SiGe [4]. The $\text{ErSi}_{1.7}$ NMOS transistor has a 15nm gate length, $I_{\text{dsat}}=190\mu\text{A}/\mu\text{m}$ at $|V_{\text{ds}}|=1.5\text{V}$. The lower NMOS I_{dsat} is due to the higher $\text{ErSi}_{1.7}$ barrier of 0.28V . Still, this is the lowest flat-band NMOS barrier achieved for a silicide. NMOS sub-threshold characteristics show a swing of $150\text{mV}/\text{dec}$, and a V_{t} of -0.1V , which can be adjusted to a higher value with the use of a mid-gap gate. The presence of the Schottky barrier can be seen in the exponential behavior of the $I_{\text{d}}-V_{\text{d}}$ plot for the NMOS devices at low V_{ds} . The gate-length dependencies of the threshold voltages and swing characteristics are shown in **Fig. 5,6** respectively. PMOS devices show excellent short channel characteristics down to 15nm gate-length, with $\Delta V_{\text{t}} = 0.2\text{V}$ and $S=100\text{mV}/\text{dec}$. NMOS devices show a similar $\Delta V_{\text{t}} = 0.2\text{V}$, but worse DIBL and $S=150\text{mV}/\text{dec}$. Since the swing

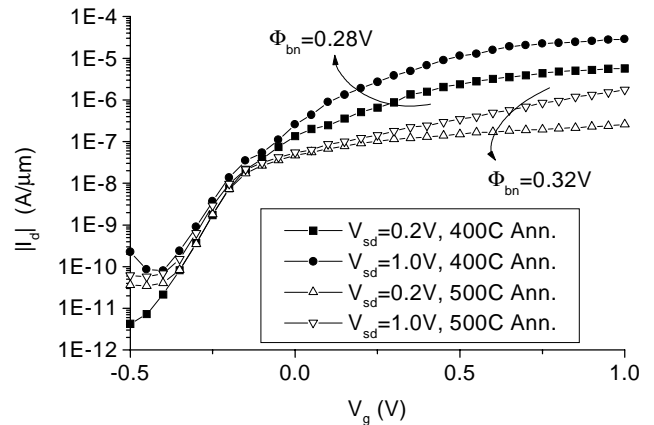


Figure 7: $I_{\text{d}}-V_{\text{g}}$ of a long channel $\text{ErSi}_{1.7}$ NMOS device before and after 500°C anneal. Silicidation temperature is 400°C .

and DIBL don't show a strong dependence on gate-length, they are probably determined by the silicon/silicide interface trap density. Annealing devices at 500°C decreases interface trap density but increases the barrier to 0.32V , **Fig. 7**. Long channel V_{t} values are -0.85V for PMOS, and 0.05V for

NMOS. These V_t values are similar to what would be expected for conventional thin-body transistors with N^+ poly gate, indicating that the low Schottky barrier doesn't inhibit current flow at threshold. The threshold data also shows that with the use of a single gate of appropriate mid-gap work-function the $|V_t|$ can be adjusted to 0.45V. While this value may be acceptable for low-power applications, it is too high for high-performance logic.

Transmission Model

As the silicide source/drain device turns on, it passes through the source-body flat-band condition, $V_g = V_{sbfb}$. This transition can be seen clearly in long channel ErSi_{1.7} devices, **Fig. 8**. For gate biases below V_{sbfb} , the Si body blocks the current flow; above V_{sbfb} , the Schottky barrier is the dominant current barrier. Below V_{sbfb} S is determined by the body potential and is ideally 60mV/dec; above the V_{sbfb} , S is determined by effective-barrier lowering mechanisms such as tunneling and image charge induction. The effective Schottky barrier, Φ_b , can be expressed as:

$$\Phi_b = \Phi_{b0} - \Delta\Phi_t - \Delta\Phi_i$$

where $\Delta\Phi_t$ and $\Delta\Phi_i$ are contributions from tunneling and image charge induction respectively, and Φ_{b0} is the source-body flat-band barrier height. Both of these lowering mechanisms depend on the lateral electric field E_y , which is proportional to the gate voltage through T_{ox} and a geometric factor G :

$$\Delta\Phi_t = \frac{1}{e} \left(\frac{3e\hbar(\ln 2)}{4\sqrt{2m^*}} \right)^{2/3} (E_y)^{2/3} \quad \text{with} \quad E_y = \frac{GV_g^*}{t_{ox}}$$

$$\Delta\Phi_i = \left(\frac{e}{4\pi\epsilon_s} \right)^{1/2} (E_y)^{1/2} \quad V_g^* = |V_g - V_{sbfb}|$$

In the subthreshold region G is an electrostatically determined constant. However, in strong inversion G decreases due to the screening of the gate field by inversion charge. Two-dimensional simulations indicate that for our structure $G \sim 0.25$ in the subthreshold region and drops to ~ 0.1 in strong inversion. With a simple transmission model the Φ_b can be translated into I_d , **Fig 9**. Our model assumes that at $\Phi_b=0$, $I_{dsat}=I_{dbal}$, the ballistic current limit[5], and employs Boltzmann statistics, which give the 60mV/dec conversion between Φ_b and I_{dsat} .

Analysis/Discussion

Using the gate work-function, G , and Φ_{b0} as fitting parameters, a fit with the data is obtained, **Fig. 10**. In PMOS devices $\Phi_{b0p}=0.22V$, slightly lower than the expected 0.24V; in NMOS devices $\Phi_{b0n}=0.28V$, the reported value for ErSi_{1.7}[6]. **Fig. 10** also indicates that for ErSi_{1.7} Φ_{b0n} changes from around 0.32V to 0.28V as the electric field at the

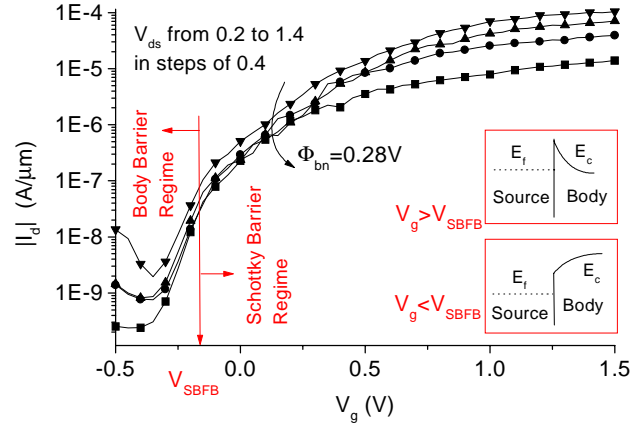


Figure 8: A 100nm NMOS device showing the two sub-threshold barrier mechanisms. Current barrier is controlled by the silicon body potential below the V_{sbfb} , and by the Schottky barrier above V_{sbfb} .

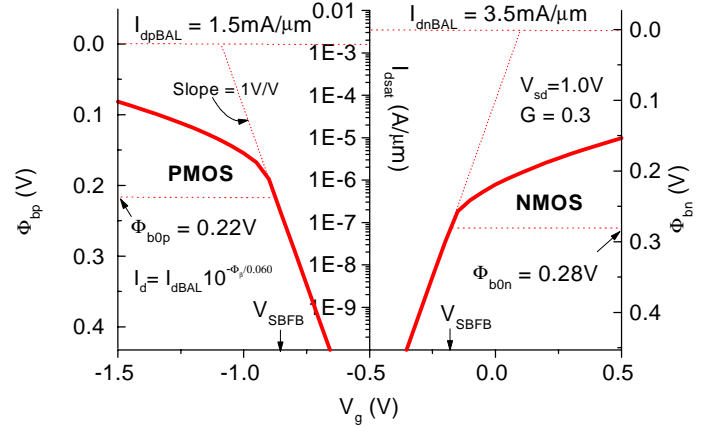


Figure 9: Construction of transmission model. Model includes barrier contributions from the silicon body, Φ_{b0} , $\Delta\Phi_t$, and $\Delta\Phi_i$. Current is derived from the barrier assuming a transmission probability of 1.

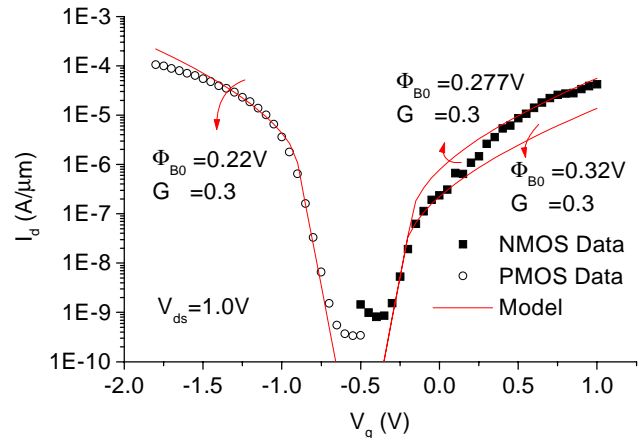


Figure 10: Barrier model fitting of 30nm wide PMOS and NMOS transistors. The G factor drops in strong inversion due to screening by the channel charge, leading to a deviation from the model at high gate biases.

interface is increased. This suggests the presence of donor states, or donor-like interface traps, at the silicide interface. With the states occupied by an electron the $\Phi_{b0n}=0.32V$, and as the electrons are removed by the gate field Φ_{b0n} changes to

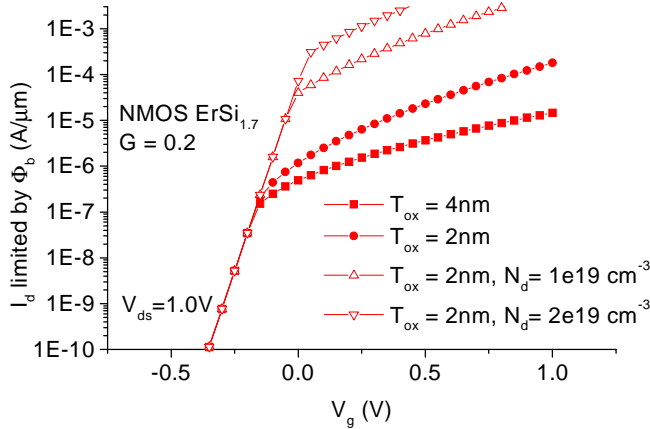


Figure 11: Investigation of the effect of oxide thickness scaling and extension doping on transmission current limit for NMOS. A conservative value of 0.2 is used for G. Reducing the oxide thickness to 20Å increases current for large V_g . A 40Å long extension doping (N-type) reduces the barrier height independently of V_g .

0.28V. This picture is consistent with the fact that Φ_{b0p} for $\text{ErSi}_{1.7}$ is 0.80V[7], indicating that the true Φ_{b0n} should be $E_g - \Phi_{b0p} = 0.32\text{V}$. At 500°C these interface states are annealed out and the Φ_{b0n} becomes 0.32V, **Fig. 7**. The presence of interface states is the likely cause of the higher variability in the NMOS device current, as well as the higher NMOS swing and DIBL values.

The I_{dsat} of our thin-body silicide source/drain devices needs to be improved to meet ITRS specifications, especially for the NMOSFET. The methods for improving device performance are: use a silicide with a lower barrier, reduce the oxide thickness, or add an extension doping to lower the barrier. Utilizing the transmission model described above, **Fig. 11** shows the effect of oxide scaling and the use of modest source/drain extension doping on the Schottky limit for I_{dsat} in NMOSFETs, assuming $G=0.2$. Oxide scaling improves I_{dsat} for $V_g > V_{\text{sbfbl}}$, since it increases the electric field

at the source/body interface. Adding an extension doping in the silicon drastically improves Schottky limit for I_{dsat} by providing a depletion layer at the source/body junction with an electric field largely independent of gate voltage, thereby directly reducing Φ_{b0} . The disadvantage of this approach is that it requires a high temperature annealing, while silicide source/drains without doping can be made below 400°C, making them compatible with a large array of gate electrode and dielectric materials. Doped source/drain devices will also show worse short channel effects, since the Schottky barrier will not be present to limit leakage current. **Fig. 12** shows the extension-doping level required to reach ITRS roadmap I_{dsat} specifications, with T_{ox} scaled to 2nm. Devices with the modest extension doping concentrations of $3\text{E}19\text{cm}^{-3}$ are projected to reach ballistic performance.

Conclusion

Complementary thin-body silicide source/drain devices with excellent turn-off characteristics have been demonstrated down to 15nm gate-length. Source/drains are fabricated from PtSi and $\text{ErSi}_{1.7}$ for PMOS and NMOS respectively. A simple transmission model fits device data and predicts that ballistic current levels can be obtained with the use of a 20Å oxide and $3\text{E}19\text{cm}^{-3}$ extension doping.

Acknowledgment: This work is supported by the DARPA AME Program, contract #N66001-97-1-8910, and the DARPA AL Program, contract #DE-AC03-76SF00098.

References

- [1] B. Yu et al., Proc. ISDRS 97, p.623-626. 1997
- [2] X. Huang et al., IEDM 99, p. 67, 1999
- [3] C. Wang et al., Appl. Phys. Lett., vol. **74** (8), p.1174, 1999
- [4] P. Hellberg et al., Elec. Dev. Lett., vol. **18**(9), p. 456, 1997
- [5] G. Timp et al., IEDM 99, p. 55, 1999
- [6] M. H. Unewisse et al., J. Appl. Phys., vol. **73**(8), p. 3873 1993
- [7] S. Vandre et al., Phys. Rev. Lett., vol. **82**(9), p.1927 1999

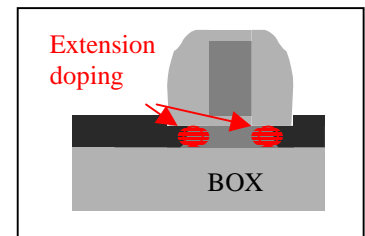
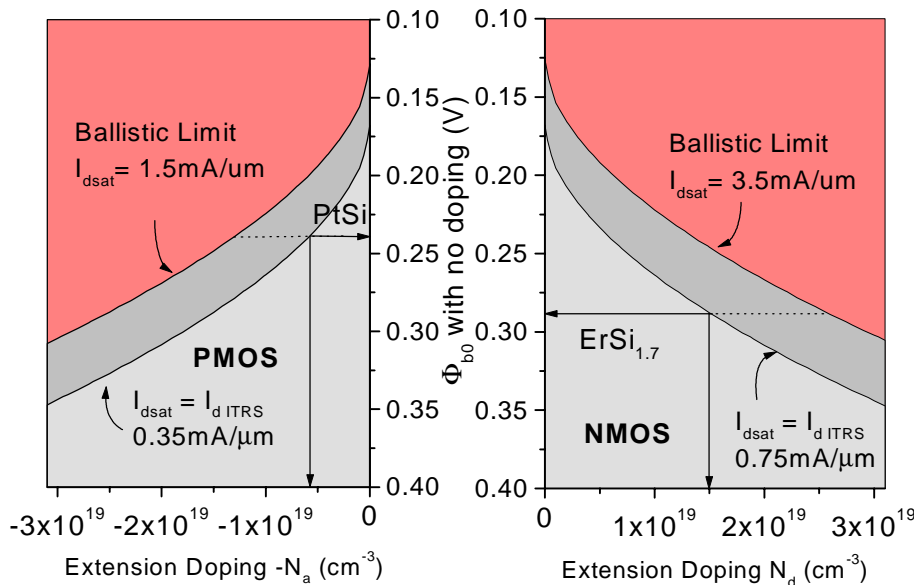


Figure 12: Contour plot of saturation current levels with $V_{\text{dd}}=1.0\text{V}$, for thin-body silicide source/drain transistors as a function of extension doping and flat-band barrier height. Strong screening is assumed, with $G=0.1$. Oxide thickness is 2nm. Ballistic current limits for both NMOS and PMOS can be reached with doping levels below $3\text{E}19\text{cm}^{-3}$.